The Cars Excitation Profile Of The MnO4- Ion Doped In KClO4

The CARS excitation profile of the MnO_4^- ion doped in $KClO_4$

Claudia Taiti, Paolo Foggi, Renato Torre and Vincenzo Schettino

Dipartimento di Chimica, Università di Firenze, via G. Capponi 9, 50121 Florence, Italy
and LENS (European Laboratory for Non-linear Spectroscopy), Largo E. Fermi 2, 50125 Forence, Italy

Received 19 May 1992; in final form 9 September 1992

The room-temperature resonance CARS spectra of the ground state ν_1 mode at 847 cm^{-1} of the permanganate ion in $KMnO_4/KClO_4$ mixed crystals at 10^{-5} mol/mol concentration as well as the CARS excitation profile for pump laser wavelengths in the 503–593 nm range are reported. The relationship between the CARS and the resonant Raman excitation profiles is discussed. Neither the build-up of excited state population nor the effect of higher- order absorption processes (two-photon transitions) are observed. It is also shown that the mechanisms affecting the room-temperature relaxation of the $^1T_2 \leftarrow {}^1A_1$ electronic transition are essentially homogeneous.

1. Introduction

Coherent anti-Stokes Raman spectroscopy (CARS) has been shown to be an efficient technique for studying molecular species at low concentration [1]. The intensity of the CARS signal is greatly enhanced when $\omega - \omega_2 = \Delta$ (where ω_1 and ω_2 are the two input laser frequencies) equals a Raman-active vibrational frequency ω_r [2]. When ω_1 approaches the frequency of an allowed electric dipole transition, a further enhancement of the signal is observed. Resonance enhancement of the CARS signal has been exploited by several authors to obtain spectra with a good signal-to-noise ratio for species at concentrations as low as 10^{-3}–10^{-7} M [3]. One-photon resonance CARS appears therefore particularly suitable to characterize impurities in crystals at concentrations where guest–guest interactions are absent. There is a renewed interest in this topic since it has been found that the vibrational dynamics (depopulation and dephasing rates) in molecular or similar crystals is greatly affected by impurities [4,5]. In this context it can be of interest to obtain information on the vibrational dynamics of the impurity itself in a host crystal [6,7]. For this purpose the sensitivity and resolution attainable at the same time with resonance CARS can be exploited.

As part of a research program on the vibrational dynamics of crystals with impurities we have undertaken a resonant CARS study of the totally symmetric stretching mode ν_1 of the permanganate ion in $KClO_4$ matrix at concentrations as low as 10^{-5} mol/mol. The choice of this system is very convenient to our purpose for several reasons. Owing to the relative dimensions of MnO_4^- and ClO_4^-, permanganate ion can easily enter as substitutional impurity in the perchlorate lattice [8]. The spectroscopy and the vibrational relaxation processes of the host crystal are well characterized by Raman [9,10], CARS [11] and infrared spectroscopy [12] and by lattice dynamics calculations [13]. The electronic properties of MnO_4^- have been investigated by resonance Raman scattering in aqueous solution [14], in KBr [15] and in $KClO_4$ [16–19] matrices. The resonant CARS spectrum of MnO_4^- is reported in water solution [20].

In this paper we report on the room-temperature resonance CARS spectra of the ν_1 mode at 847 cm^{-1} of the permanganate ion in $KMnO_4/KClO_4$ mixed crystals as well as the CARS excitation profile (CEP) for pump laser wavelengths in the 503–593 nm range. In this range the ω_1 frequency is in resonance with the $^1T_2 \leftarrow {}^1A_1$ electronic transition centered at 19000

Correspondence to: P. Foggi, Dipartimento di Chimica, Università di Firenze, via G. Capponi 9, 50121 Florence, Italy.

cm^{-1}, which shows a clearly resolved vibronic structure.

CEPs are defined as the dependence on ω_1 of the square modulus of the fully resonant part of the CARS susceptibility at a constant value of $\Delta=\omega_r$. They are obtained by measuring the intensity of the CARS signal as ω_1 varies inside the one-photon absorption profile. The study of CARS excitation profiles is of interest intrinsically since, through it, one can obtain important pieces of information (such as molecular geometry, lifetime of vibronic levels, etc.) on the electronic states of the sample [21]. In the present case the purpose of the excitation profile analysis originated from the need to define the most appropriate conditions to study the linewidth of the Raman transition. Many experimental and theoretical studies have dealt with resonant CARS processes [3]. However, only few of them have directly addressed the question of the relation existing between CEPs and Raman excitation profiles (REPs) [22,23]. Comparison of CEPs and REPs measured under the same experimental conditions can provide an additional piece of information on line broadening mechanisms in the excited state, specifically on the contribution of inhomogeneous effects [23]. The Raman excitation profile has already been reported for the $KMnO_4/KClO_4$ system [16]. Comparison of the latter with the CARS excitation profile obtained in the present Letter shows that line broadening in $KMnO_4/KClO_4$ is essentially homogeneous.

2. Experimental

Single crystals of good optical quality were grown from aqueous solutions saturated in $KClO_4$ and 10^{-3} M in $KMnO_4$, using Merck reagents. The actual concentration of the permanganate ion in the matrix was then determined using the following procedure. Pieces of the sample were weighted and then dissolved in water. The absorbance of these solutions was compared to that of MnO_4^- standard solutions. The concentration of MnO_4^- was found to be 10^{-5} mol/mol. Crystals were cut orthogonal to the principal optical directions, which were determined with the aid of a polarizing microscope. Room temperature Raman spectra of the matrix in various scattering geometries were found to be coincident with those already reported [10], allowing the identification of the crystal axes. These spectra were obtained by using a standard Raman apparatus with excitation by the 514 nm line of an argon-ion laser and photon-counting detection.

Measurements of the CARS spectra were performed by using a standard configuration with planar phase-matching geometry. The experimental has been described in a previous paper [24]. The crystals were mounted on a holder in such a way that the laser beams, polarized parallel to the direction of the a crystallographic axis, propagated along the c axis corresponding to the thinner edge of the crystal. The small sample thickness and an appropriate choice of the crystal spot made possible to obtain intense CARS signals free from any background due to scattered light. The experimental set up was optimized on the CARS signal relative to the totally-symmetric vibrational mode ν_1 at 940 cm^{-1} of perchlorate molecule taken as an internal standard. The low dispersion of the $KClO_4$ index of refraction guarantees that the phase-matching conditions are the same over more than 200 cm^{-1}. For this reason, at each value of the ω_1 frequency the same phase-matching conditions were used for recording the spectra both of the $940_{(ClO_4^-)}$ cm^{-1} and the $847_{(MnO_4^-)}$ cm^{-1} vibrational modes, such that the active volume of the sample and the absorption of the lasers and signal beams were not modified.

3. Results and discussion

In fig. 1 some examples of the MnO_4^- ion CARS spectra at different λ_1 wavelength values and the relative fits are shown. It can be seen that the CARS lineshape changes considerably as the pump frequency is tuned through the absorption band of the MnO_4^- ion. Such a complex lineshape has been observed in resonance CARS [3] and interpreted in terms of interference between various contributions to $\chi^{(3)}$ The intensity of the CARS signal is proportional to the square modulus of the third-order susceptibility $\chi^{(3)}$, which can be expressed as the sum of a non-resonant and a Raman resonant part:

$$\chi^{(3)}=\chi_{NR}^{(3)}+\chi_{R}^{(3)}\,. \qquad (1)$$

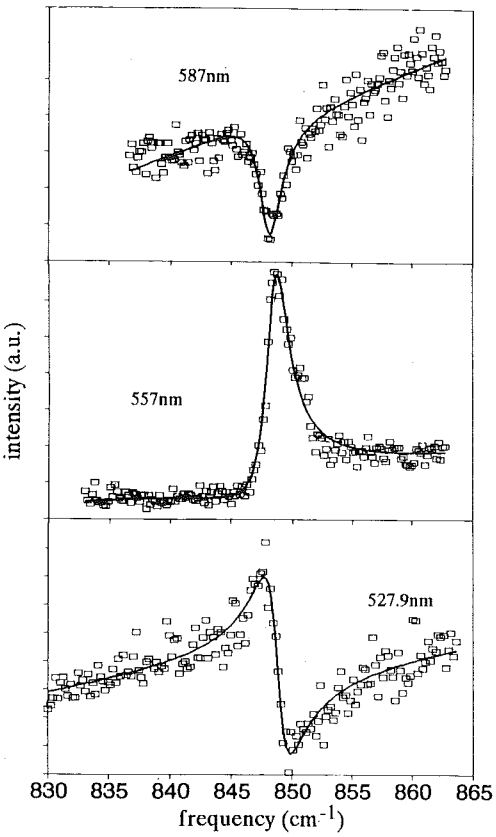

Fig. 1. Some examples of the MnO_4^- ν_1 CARS spectra at different λ_1 wavelength values. (□) Experimental data and (——) fit.

The non-resonant contribution $\chi_{NR}^{(3)}$ includes all electronic and vibrational transitions terms out of resonance (background signal) and it is generally a slowly varying function of the frequency difference $\omega_1-\omega_2=\Delta$. When $\Delta=\omega_r$, the sum is dominated by the complex Raman susceptibility $\chi_R^{(3)}$. In the case of a single isolated Raman resonance and under one-photon resonance conditions, $\chi^{(3)}$ can be expressed as [20]:

$$\chi^{(3)}=B+\frac{R_r+iI_r}{\delta_r-i\Gamma_r}, \qquad (2)$$

where the non-resonant background B is real if no two-photon resonance is excited. In eq. (2) $\delta_r=\omega_r-\Delta$ is the frequency mismatch, R_r and I_r are the real and imaginary parts of the Raman susceptibility $\chi_R^{(3)}$, respectively, and Γ_r is the Raman transition half-width at half-maximum (hwhm). In the present case the choice of eq. (2) is justified because the ν_1 mode of MnO_4^- is well separated from all the other modes of the mixed crystal, the closest Raman active mode being $\approx 70\ cm^{-1}$ at higher frequency ($2\nu_2$ of $KClO_4$).

The intensity of the CARS signal is then

$$|\chi^{(3)}|^2=B^2+\frac{R_r^2+I_r^2}{\delta_r^2+\Gamma_r^2}+\frac{2BR_r\delta_r}{\delta_r^2+\Gamma_r^2}-\frac{2BI_r\Gamma_r}{\delta_r^2+\Gamma_r^2}. \qquad (3)$$

Eq. (3) was used to fit the experimental CARS spectra with a least-squares fitting program based on the Marquardt algorithm and considering B, R_r, I_r and Γ_r as variable parameters. Examples of the fit are shown in fig. 1. In the present case B was found to be a slowly varying function of the frequency ω_1. At present our instrumental sensitivity does not allow us to observe measurable variations of B passing from the pure $KClO_4$ crystal to the mixed one. We have also verified that B has no imaginary contributions; within the experimental error there is no evidence of two-photon electronic transitions. The wide variety of lineshapes is due to the cross terms between resonant and non-resonant contributions. Using the fitting procedure described above the square modulus of the third-order susceptibility was obtained as a function of the wavelength of the ω_1 beam. The results are shown in fig. 2 where the CARS excitation profile is compared with the one-photon absorption spectrum and the resonance Raman excitation profile [16]. It can be seen that the CEP exhibits a well defined peak centered at 557 nm, and a weaker feature at shorter wavelengths extending up to 515 nm. It is apparent from fig. 2 that the electronic origin of the absorption spectrum, of the REP and of the CEP are coincident.

The connection between CARS and Raman excitation profiles has been discussed by Lukashin and Frank-Kamenetskii [23]. It has been shown that, for systems with an initial population in the ground state only and with no inhomogeneous electronic transition line broadening, CEP $C(\omega_1)$ can be expressed simply as the product of two REPs $R(\omega_1)$ and $R(\omega_1+\omega_r)$ shifted in frequency by an amount corresponding to the Raman transition ω_r:

$$C(\omega_1)=R(\omega_1)\,R(\omega_1+\omega_r)\,. \qquad (4)$$

Eq. (4) has been applied in the present case to reproduce the experimental CEP starting from REP

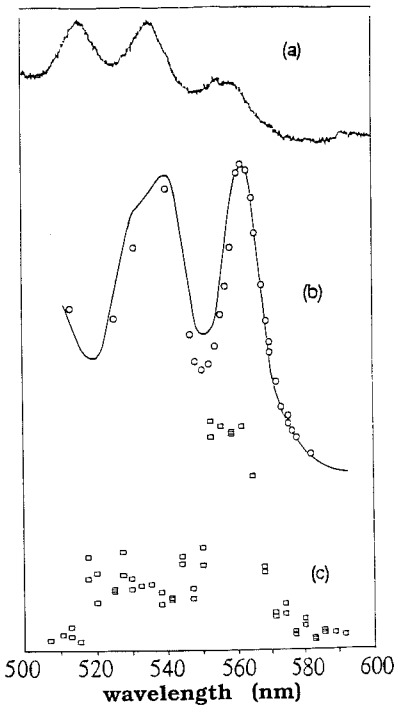

Fig. 2. Absorption spectrum (a), REP from ref. [16] (b), and CEP (c) of the ν_1 vibrational mode at 847 cm^{-1} of the permanganate ion in $KMnO_4/KClO_4$ mixed crystal.

values previously reported [16]. The experimental REP of the ν_1 mode of the MnO_4^- ion in $KClO_4$/$KMnO_4$ mixed crystal was well reproduced using the following quantum mechanical expression:

$$R(\omega_1)\propto \sum_v |A_v|^2\left(\frac{1}{\epsilon_v^2+\Gamma_v^2}+\frac{2(\epsilon_v\epsilon_v^*+\Gamma_v^2)}{(\epsilon_v^2+\Gamma_v^2)(\epsilon_v^{*2}+\Gamma_v^2)}+\frac{1}{\epsilon_v^{*2}+\Gamma_v^2}\right)$$
$$+2\sum_{v<v'}\sum_{v'} A_vA_{v'}\left(\frac{\epsilon_v\epsilon_v^*+\Gamma_v\Gamma_{v'}}{(\epsilon_v^2+\Gamma_v^2)(\epsilon_{v'}^2+\Gamma_{v'}^2)}+\frac{\epsilon_v\epsilon_{v'}^*+\Gamma_v\Gamma_{v'}}{(\epsilon_v^2+\Gamma_v^2)(\epsilon_{v'}^{*2}+\Gamma_{v'}^2)}\right.$$
$$\left.+\frac{\epsilon_v^*\epsilon_{v'}+\Gamma_v\Gamma_{v'}}{(\epsilon_v^{*2}+\Gamma_v^2)(\epsilon_{v'}^2+\Gamma_{v'}^2)}+\frac{\epsilon_v^*\epsilon_{v'}^*+\Gamma_v\Gamma_{v'}}{(\epsilon_v^{*2}+\Gamma_v^2)(\epsilon_{v'}^{*2}+\Gamma_{v'}^2)}\right) \quad (5)$$

derived in the BO and Condon approximations. In eq. (5) $|n\rangle$ and $|v\rangle$ are the vibrational sublevels of the fundamental $|g\rangle$ and excited $|e\rangle$ electronic states, respectively, Γ_v is the hwhm of the $|v\rangle$ sublevel and

$$\epsilon_v=E_{e(v)}-E_{g(0)}-hc\nu_1\,,$$
$$\epsilon_v^*=E_{e(v)}-E_{g(n)}+hc\nu_1\,,$$
$$E_{e(v)}-E_{g(n)}=hc\nu_{00}+vhc\nu'-nhc\nu''\,,$$
$$|A_v|^2=(\langle n|v\rangle\langle v|0\rangle)^2\,,$$
$$A_vA_{v'}=\langle n|v\rangle\langle v|0\rangle\langle n|v'\rangle\langle v'|0\rangle\,,$$

where $\langle v|n\rangle$ are the Franck–Condon overlap integrals calculated in the harmonic approximation. The best fitting parameters and the overlap integrals obtained from the REP [16] are reported in table 1. Using this set of parameters without any further adjustment, the CEP for the ν_1 mode of MnO_4^- has been calculated. The calculated CEP, multiplied by a constant scaling factor to account for the instrumental responsivity, is shown in fig. 3 and compared with the experimental one. The agreement between the experimental points and the calculated curve is good. As already discussed [22], deviations of the CEP from eq. (4) provide a possible mean of identifying the presence of inhomogeneous effects without resorting to any specific model for homogeneous broadening. It must be pointed out that other effects can contribute to the broadening of the CEP peaks. For example, one should include in the model contributions from Herzberg–Teller terms in order to calculate a more general expression for $R(\omega_1)$. However, as already observed [16], the region of the 0–0 peak in the excitation profile of MnO_4^- is the least affected by interference effects. Therefore the conclusions of the present discussion about broad-

Table 1
Parameters and Franck–Condon overlap integrals from ref. [16] used to calculate the CEP of the $KMnO_4/KClO_4$ system (see eqs. (4) and (5))

Parameters	Values	n/v	$\langle 0\|v\rangle$	$\langle 1\|n\rangle$
ν_{00} (cm^{-1})	17950	0	0.4522	0.5499
		1	−0.5880	−0.2640
ν_1' (cm^{-1})	847	2	0.5193	−0.1981
		3	−0.3578	0.4623
ν_1'' (cm^{-1})	740	4	0.2026	−0.4676
		5	−0.0964	0.3347
Γ/hc (cm^{-1})	300	6	−0.0388	−0.1885

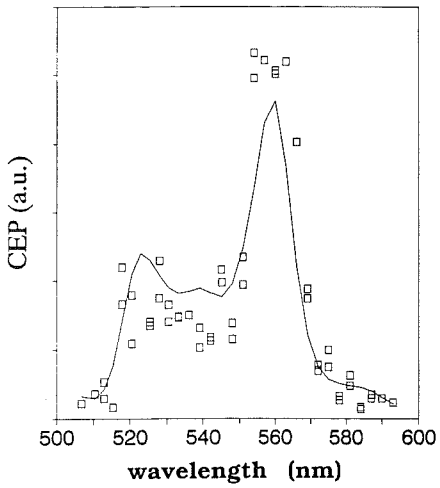

Fig. 3. Comparison between the experimental (□) and calculated (——) CEP of the ν_1 vibrational mode at 847 cm^{-1} of the permanganate ion in $KMnO_4/KClO_4$ mixed crystal (see text).

ening mechanisms in the electronic excited state hold at least for the 0–0 peak of the CEP.

A further proof of the agreement between calculations and experimental data is shown in fig. 4 where the real and imaginary parts of $\chi_R^{(3)}$ are reported separately. The position of the observed minimum of the real part and of the maximum of the imaginary part are coincident, within experimental error, with the calculated ones. There is only a difference in the calculated and observed minimum intensity of the real part. It is important to stress again that no fitting procedures were included in the calculation. As can be seen from fig. 3, the experimental linewidth of the main peak is well reproduced in the calculated CEP. From these results it can be concluded that the relaxation mechanisms affecting the linewidth of the $^1T_2 \leftarrow {}^1A_1$ electronic transition in $KClO_4/KMnO_4$ are essentially homogeneous, at least at room temperature.

The possibility of interpreting our results in a straightforward manner is mainly due to the fact that the lifetime of the electronic excitation is rather fast at room temperature. No build-up of an excited-state population is observed and the fit of the resonant CARS spectra do not require the introduction of higher-order contributions to the overall susceptibility as instead observed in the case of some organic compounds [22]. Our results are consistent with the

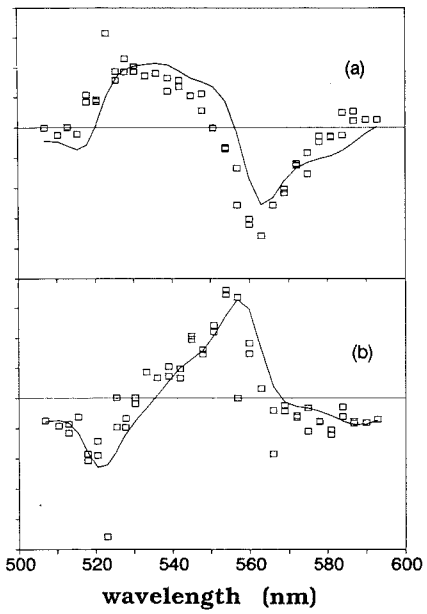

Fig. 4. Real (a) and immaginary (b) part of the $\chi^{(3)}_{CARS}$ of the ν_1 vibrational mode at 847 cm^{-1} of the permanganate ion in $KMnO_4/KClO_4$ mixed crystal. (□) Experimental and (——) calculated (see text).

estimate of the relaxation time T_1 from fluorescence measurements. A $T_1 = 10^{-13}$ s and a low fluorescence quantum yield prove the presence of an efficient radiationless transition [19].

4. Conclusions

We have reported the results of an investigation of the resonance CARS spectra and excitation profile of the MnO_4^- ν_1 vibrational mode in $KClO_4$ at room temperature. This work is one of the first examples of CEPs of isolated species in a crystalline matrix. It has been verified that, within experimental error, our results are well reproduced by the Lukashin and Frank–Kamenetskii theory under the hypothesis of homogeneous broadening.

Acknowledgement

This work is supported by the Italian Consiglio Nazionale delle Ricerche (CNR), PG-MSTA. The

authors wish to thank Professor R. Bozio for helpful discussions. One of the authors (CT) thanks Dr. R. Bini for his suggestions.

References

[1] G.I. Eesley, Coherent Raman spectroscopy (Pergamon Press, Oxford, 1981).
[2] Y.R. Shen, The principles of nonlinear optics (Wiley, New York, 1984).
[3] L.A. Carreira, T.C. Maguire and T.B. Malloy Jr., J. Chem. Phys. 66 (1977) 2621;
P.K. Dutta, R. Dallinger and T.G. Spiro, Chem. Phys. 73 (1980) 3580.
[4] J. Trout, S. Velsko, R. Bozio, P. Decola and R.M. Hochstrasser, J. Chem. Phys. 81 (1985) 4746.
[5] M. Becucci, P. Foggi, E. Castellucci, S. Califano and D.A. Dows, J. Chem. Phys. 96 (1992) 98.
[6] A.J. Barnes, W.J. Orville-Thomas and A. Müller, eds., Matrix isolation spectroscopy, Nato Advanced Study Institutes Series C, Vol. 76 (Reidel, Dodrecht, 1981).
[7] F. Legay, in: Chemical and biochemical applications of lasers, Vol. 2, ed. C.B. Moore (Academic Press, New York, 1977) p. 43.
[8] G.B. Johansson and O. Lindqvist, Acta Crist. B 33 (1977) 298.
[9] H.D. Lutz, R.A. Becker, B.G. Hoelscher and H.J. Berthold, Spectrochim. Acta 39A (1983) 7.
[10] N. Toupry, H. Poulet, M. LePostollec, R.M. Pick and M. Yvinec, J. Raman Spectry. 14 (1983) 166.
[11] R. Righini, L. Angeloni, P. Foggi, E. Castellucci and S. Califano, Chem. Phys. 131 (1989) 463.
[12] R. Bini, P. Foggi, P.R. Salvi and V. Schettino, J. Phys. Chem. 94 (1990) 6653.
[13] G. Signorini, R. Righini and V. Schettino, Chem. Phys. 154 (1991) 245.
[14] W. Kiefer and H.J. Bernstein, Mol. Phys. 23 (1972) 835.
[15] L.A. Rebane and A.A. Khaav, Soviet Phys. Solid State 28 (1986) 574.
[16] R.G.H. Clark and B. Stewart, J. Am. Chem. Soc. 103 (1981) 6593.
[17] L.A. Rebane, J. Phys. (Paris) 46 (1985) C7-435.
[18] A.A. Khaav, K.E. Khaller, I.Yu. Tekhver and L.A. Rebane, Soviet Phys. Solid State 26 (1984) 1972.
[19] L.A. Rebane and G.E. Blumberg, J. Luminescence 40 (1988) 599.
[20] L.A. Carreira and R.R. Antcliff, in: Advances in laser spectroscopy, Vol. 1, eds. B.A. Garetz and J.R. Lombardi (Heyden, London, 1982) p. 121.
[21] L.A. Carreira, L.P. Goss and T.B. Malloy Jr., in: Chemical applications of nonlinear Raman spectroscopy, ed. A.B. Harvey (Academic Press, New York, 1981) p. 321.
[22] A. Feis, C. Ferrante and R. Bozio, Chem. Phys. Letters 175 (1990) 156.
[23] A.V. Lukashin and M.D. Frank-Kamenetskii, J. Raman Spectry. 12 (1982) 234.
[24] R. Bini, P. Foggi, G. Marconi and E. Castellucci, J. Luminescence 53 (1992) 541.